A range of voltage-clamp protocol designs for rapid capture of hERG kinetics

Chon Lok Lei[1,2], Dominic G. Whittaker[3], Monique J. Windley[4,5], Matthew D. Perry[6], Adam P. Hill[4,5], Gary R. Mirams[3]

[1]Institute of Translational Medicine, Faculty of Health Sciences, University of Macau, Macau
[2]Department of Biomedical Sciences, Faculty of Health Sciences, University of Macau, Macau
[3]Centre for Mathematical Medicine & Biology, School of Mathematical Sciences, University of Nottingham, Nottingham, United Kingdom
[4]Computational Cardiology Laboratory, Victor Chang Cardiac Research Institute, Darlinghurst, New South Wales, Australia
[5]School of Clinical Medicine, Facility of Medicine and Health, University of New South Wales Sydney, New South Wales, Australia
[6]School of Biomedical Sciences, Faculty of Medicine and Health, University of New South Wales Sydney, New South Wales, Australia

Abstract

We provide details of a series of short voltage-clamp protocols designed for gathering a large amount of information on hERG (K_v11.1) ion channel gating. The protocols have a limited number of steps and consist only of steps and ramps, making them easy to implement on any patch clamp setup, including automated platforms. The primary objective is to assist with parameterisation, selection and refinement of mathematical models of hERG gating. We detail a series of manual and automated model-driven designs, together with an explanation of their rationale and design criteria. Although the protocols are intended to study hERG1a currents, the approaches could be easily extended and generalised to other ion channel currents.

1 Introduction

This report describes a series of voltage-clamp protocol waveforms that were designed to explore the gating of cell lines expressing hERG1a / K_v11.1 channels, which are the primary subunit of the channels carrying the cardiac rapid delayed rectifier potassium current, I_{Kr} (Sanguinetti et al., 1995; Vandenberg et al., 2012).

The aim is to build on our previous studies that aimed to develop a range of short, information-rich voltage clamp protocols to use in experimental recordings to capture hERG gating behaviour (Beattie et al., 2018; Lei et al., 2019b). Here we extend these to a wide range of protocols to better parameterise, select and test mathematical models of hERG gating (Bett et al., 2011) and in particular to gain a better understanding and quantification of model discrepancy — when models cannot correctly predict what happens in reality (Shuttleworth et al., 2024). As a result, some protocols will focus on classic optimal experimental design in terms of reducing uncertainty / improving identifiability of model parameter estimates (Lei et al., 2023). Whilst others focus on maximising differences between trained models to assist in model selection/discrimination.

All these protocols were designed during the Isaac Newton Institute's Fickle Heart programme in May–June 2019 (Mirams et al., 2020). The protocols are all designed to be run on an automated patch platform, namely the Nanion SyncroPatch384PE (Obergrussberger et al., 2016), which at the time had a restriction of only allowing up to 64 commands (steps or ramps) to define a single voltage-clamp protocol.

2 Models used in protocol design process

Our designs are model-driven akin to Lei et al. (2023), where mathematical models are used as part of automatic optimal design; even where our designs are manual they were done by visually examining the results of forward simulations.

The model structures that we used here are Beattie et al. (2018) and Wang et al. (1997) (also used in Fink et al. (2008)), with their Markov diagrams shown in Figure 1. The first model (Beattie et al., 2018) is a Hodgkin-Huxley style model with two independent gates, which can be represented as a symmetric 4-state Markov model (Rudy and Silva, 2006, Fig. 4B). The second model Wang et al. (1997) is a 5-state Markov model with 3 closed states, an open state, and an inactivated state connected sequentially.

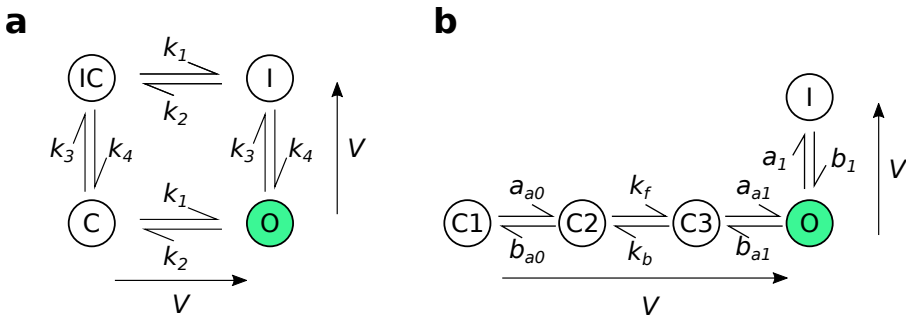

Figure 1: The model structures used for experimental design. (**a**): the four-state Beattie et al. (2018) model. (**b**): the five-state Wang et al. (1997) model. The arrows adjacent to each model structure indicate the direction in which rates increase as the voltage increases. Reproduced from Shuttleworth et al. (2024) under a CC-BY licence.

2.1 Beattie model

In matrix/vector form, the Beattie et al. (2018) model can be written as,

$$\frac{\mathrm{d}\mathbf{x}}{\mathrm{d}t} = \begin{bmatrix} -k_1 - k_3 & 0 & k_4 & k_2 \\ 0 & -k_2 - k_4 & k_1 & k_3 \\ k_3 & k_2 & -k_1 - k_4 & 0 \\ k_1 & k_4 & 0 & -k_2 - k_3 \end{bmatrix} \mathbf{x}, \tag{1}$$

where

$$\mathbf{x} = \left[C,\ I,\ IC,\ O\right]^T,$$

and

$$\begin{aligned} k_1 &= p_1 e^{p_2 V}, \\ k_2 &= p_3 e^{-p_4 V}, \\ k_3 &= p_5 e^{p_6 V}, \\ k_4 &= p_7 e^{-p_8 V}. \end{aligned}$$

This model is equivalent to a two gate Hodgkin-Huxley style gating model with open probability given by an "activation" a gate representing the 'right' transitions in Fig. 1a multiplied by an "inactivation" r gate representing the 'down' transitions (Clerx et al., 2019a; Mirams, 2023), so in the below designs when we refer to "Hodgkin-Huxley" (HH) it is this interpretation of the model we are using.

2.2 Wang model

The Wang et al. (1997) model can be written as:

$$\frac{\mathrm{d}\mathbf{x}}{\mathrm{d}t} = \begin{bmatrix} -a_{a0} & b_{a0} & 0 & 0 & 0 \\ a_{a0} & -b_{a0} - k_f & k_b & 0 & 0 \\ 0 & k_f & -k_b - a_{a1} & b_{a1} & 0 \\ 0 & 0 & a_{a1} & -b_{a1} - a_1 & b_1 \\ 0 & 0 & 0 & a_1 & -b_1 \end{bmatrix} \mathbf{x}, \tag{2}$$

where

$$\mathbf{x} = \begin{bmatrix} C_1, & C_2, & C_3, & O, & I \end{bmatrix}^T,$$

and

$$\begin{aligned} a_1 &= q_1 e^{q_2 V}, \\ a_{a0} &= q_3 e^{q_4 V}, \\ a_{a1} &= q_5 e^{q_6 V}, \\ b_{a1} &= q_7 e^{-q_8 V}, \\ b_1 &= q_9 e^{-q_{10} V}, \\ b_{a0} &= q_{11} e^{-q_{12} V}. \end{aligned}$$

The default (room temperature) parameter values for both models are presented in Table 1. In practice we remove one state from the system and set it equal to "one minus the sum of the rest" to solve the ODE system, to improve numerical stability. All models are solved using a Python package Myokit (Clerx et al., 2016) using SUNDIALS CVODE (Hindmarsh et al., 2005).

Wang model

	Value	Range	Units
g	1.52	—	$\times 10^{-1}$ μS
k_b	3.68	$[0.67, 99993]$	$\times 10^{-2}$ ms^{-1}
k_f	2.38	$[1.31, 99550]$	$\times 10^{-2}$ ms^{-1}
q_1	9.08	$[12.4, 18.1]$	$\times 10^{-2}$ ms^{-1}
q_2	2.34	$[1.55, 2.06]$	$\times 10^{-2}$ mV^{-1}
q_3	2.23	$[0.03, 1.02]$	$\times 10^{-2}$ ms^{-1}
q_4	1.18	$[0.0001, 10.9]$	$\times 10^{-2}$ mV^{-1}
q_5	1.37	$[0.23, 364]$	$\times 10^{-2}$ ms^{-1}
q_6	3.82	$[0.0001, 6.44]$	$\times 10^{-2}$ mV^{-1}
q_7	6.89	$[12.9, 76.9]$	$\times 10^{-5}$ ms^{-1}
q_8	4.18	$[0.29, 0.39]$	$\times 10^{-2}$ mV^{-1}
q_9	6.50	$[3.55, 5.75]$	$\times 10^{-3}$ ms^{-1}
q_{10}	3.27	$[2.89, 3.34]$	$\times 10^{-2}$ mV^{-1}
q_{11}	4.70	$[0.007, 1458]$	$\times 10^{-2}$ mV^{-1}
q_{12}	6.31	$[1.16, 11.8]$	$\times 10^{-2}$ ms^{-1}

Beattie model

	Value	Range	Units
g	1.52	—	$\times 10^{-1}$ μS
p_1	2.26	$[1.39, 12.9]$	$\times 10^{-4}$ ms^{-1}
p_2	6.99	$[1.08, 8.49]$	$\times 10^{-2}$ mV^{-1}
p_3	3.45	$[2.77, 32.3]$	$\times 10^{-5}$ ms^{-1}
p_4	5.46	$[2.48, 4.56]$	$\times 10^{-2}$ mV^{-1}
p_5	8.73	$[6.40, 19.9]$	$\times 10^{-2}$ ms^{-1}
p_6	8.91	$[21.8, 38.7]$	$\times 10^{-3}$ mV^{-1}
p_7	5.15	$[7.07, 10.9]$	$\times 10^{-3}$ ms^{-1}
p_8	3.16	$[2.89, 3.39]$	$\times 10^{-2}$ mV^{-1}

Table 1: The default parameter sets we use for the Wang et al. (1997) and Beattie et al. (2018) models. The same maximal conductance (g) is used for both models. The column 'Range' indicates the parameter range obtained from real data fitting results based on protocols staircaseramp, sis, hh3step, and wang3step, which is used for global sensitivity-based designs.

3 Common protocol segments

As described in Mirams et al. (2024), all the protocols we have designed have a common start and end sections defined in Table 2. The purposes of these are

- Start — an 'activation step' to provoke a very large tail current and help with conductance estimation, as discussed in Beattie et al. (2018).
- End — a 'reversal ramp' to help assess whether the current is reversing at the expected Nernst potential, discussed in Lei et al. (2019b).
- both can also be used in quality control to check that these sections behave similarly over time when different protocols are applied to the same cell.

Table 2: Reproduced from Mirams et al. (2024). Details of the Start and End clamp sections for all designs. 't' indicates the duration of the clamp section, and 'V' the relevant voltage(s) for this clamp. Where 'Ramp' is specified it is a linear ramp over time between the voltages shown, as opposed to a constant voltage clamp for a 'Step'.

Clamp	Initial: for leak and conductance			End: reversal ramp sequence		
#	Step/Ramp	t (ms)	V (mV)	Step/Ramp	t (ms)	V (mV)
1	Step	250	−80	Step	1000	−80
2	Step	50	−120	Step	500	40
3	Ramp	400	−120 to −80	Step	10	−70
4	Step	200	−80	Ramp	100	−70 to −110
5	Step	1000	40	Step	390	−120
6	Step	500	−120	Step	500	−80
7	Step	1000	−80	—	—	—

4 Manual protocol designs

The details of the protocols in this section are provided in Table 3.

4.1 Original staircase protocol

Figure 2 shows the original staircase protocol. It was manually designed to capture various dynamics of hERG (Lei et al., 2019b,a), which has been used and tested on the Nanion SyncroPatch384PE. We have been using it as a quality control of the full run of the experiments when designing the protocols in the rest of this report.

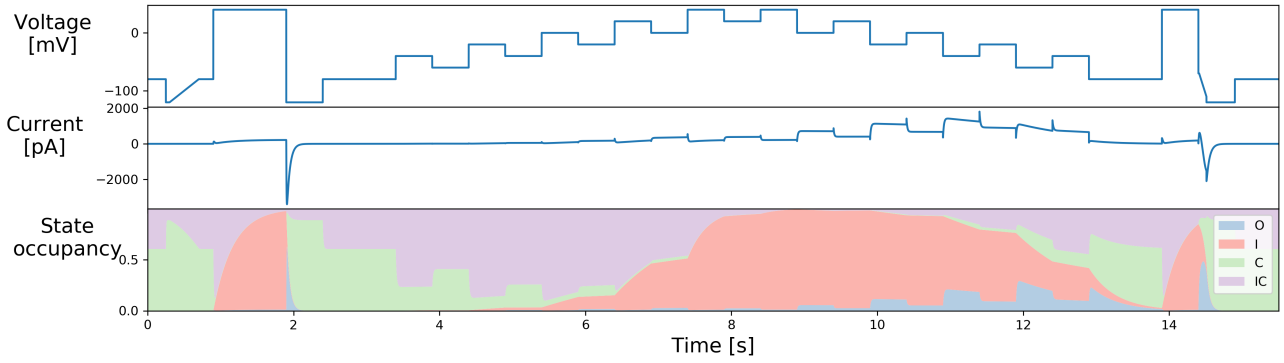

Figure 2: The staircase protocol and its simulation, with state occupancy shown for the Beattie et al. (2018) model of Fig. 1a. Reproduced from (Lei et al., 2019b) under a CC-BY licence.

4.2 Staircase-in-staircase protocol

The original staircase protocol provided a good foundation and motivation for improving experimental designs for characterisation of ion channel kinetics in high-throughput machines. We attempted to

further improve this manual design by enhancing the exploration of inactivation processes of hERG. The original staircase protocol involves only voltage steps of 500 ms, which may not be able to explore fully the fast dynamics of hERG inactivation processes. Therefore, a shorter step duration version (50 ms) of the full staircase protocol is introduced at the middle of the staircase protocol, termed the staircase-in-staircase (sis) protocol (Figure 3). We also explored the possibility of inverting the order of the staircase as shown in Figure 4 (sisi).

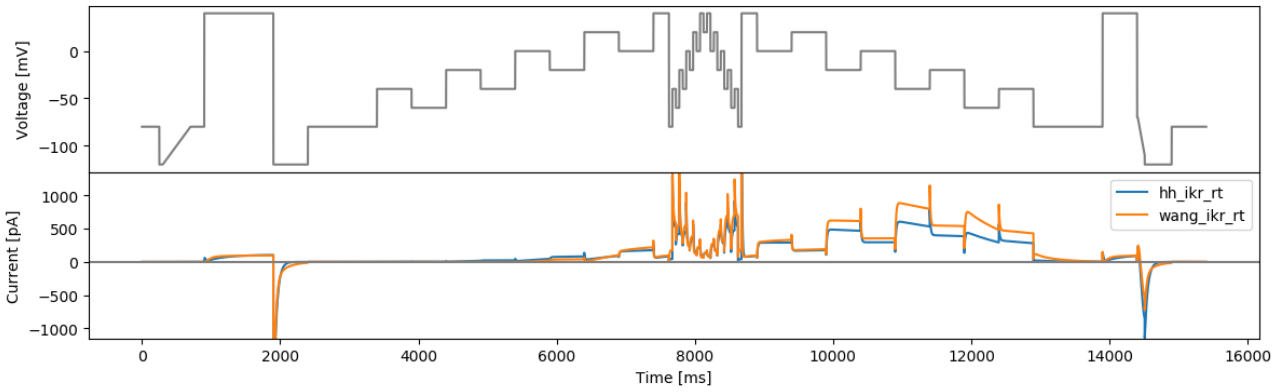

Figure 3: The staircase-in-staircase (sis) protocol and simulated currents from both models. (`hh_ikr_rt` is the Beattie et al. (2018) model of I_{Kr} and `wang_ikr_rt` is the Wang et al. (1997) model of I_{Kr}, both parameterised to room temperature data).

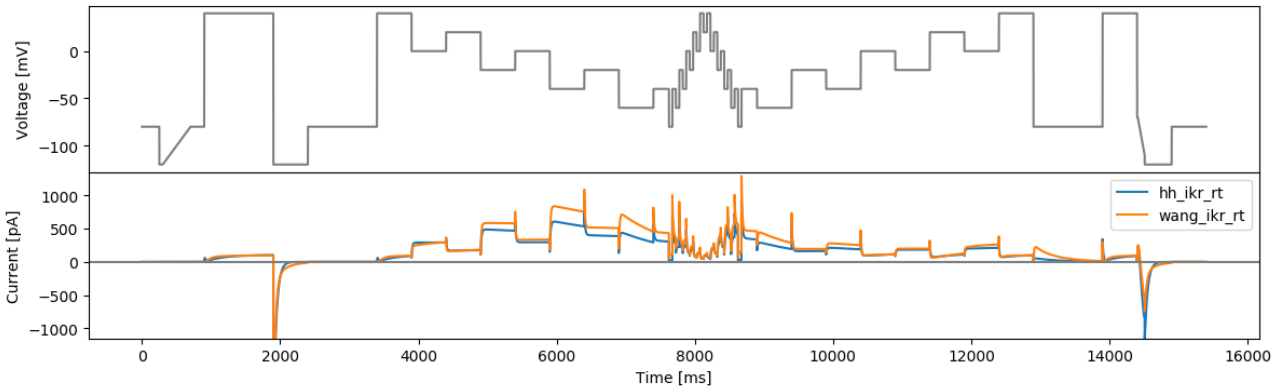

Figure 4: The inverted staircase-in-staircase (sisi) protocol and simulated currents from both models

4.3 Phase-space filling protocol

The idea here is to have a protocol that fills up the phase-voltage space as much as possible. In brief, this design draws out the a, r, V three dimensional 'phase-voltage space' $\{[0,1],[0,1],[-120,60]\}$ for the Beattie et al. (2018) model and subdivides it into 6 compartments in each dimension, giving a total of $N = 6^3 = 216$ boxes. Since the phase space defines all possible behaviours of a model, if a protocol forces the model to visit as many of these boxes as possible, then the observations should test model assumptions well and provide rich information to fit model parameters. We have published the rationale and details of the design process for these protocol separately in Mirams et al. (2024). Figure 5 shows a manually-tuned phase space filling protocol (manualppx); no objective function *per se*.

4.4 A square-wave conversion of the sinusoidal protocol

In this design, we aim to design protocols based on sums of square waves, as inspired by Beattie et al. (2018). Such a protocol consists of a combination of N square waves, where each square wave i is

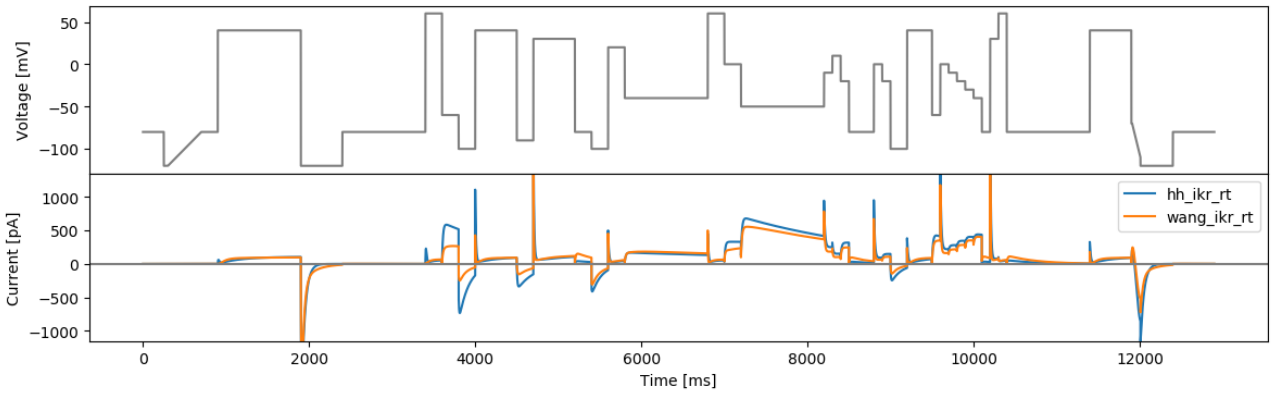

Figure 5: The manual phase space protocol (manualppx) and simulated currents from both models.

defined by amplitude a_i, (angular) frequency ω_i, and phase lag ϕ_i. The protocol is defined by $3N$ parameters plus an extra parameter for an offset voltage, which can be expressed as:

$$V_{\text{square wave}}(t) = b + \sum_{i}^{N} a_i \,\text{sign}\left(\sin(\omega_i t + \phi_i)\right), \tag{3}$$

where the function sign$(\cdot)$ takes a value $+1$ if its argument is positive, -1 if negative, or 0 if the argument is 0.

A direct conversion of the sine waves in the Beattie et al. (2018) protocol is performed, with the same amplitudes and frequencies, to square waves. It is a combination of three square waves ($N = 3$) with a_1 =54 mV, a_2 =26 mV, a_3 =10 mV, ω_1 =0.007 ms^{-1}, ω_2 =0.037 ms^{-1}, ω_3 =0.19 ms^{-1}, and $\phi_1 = \phi_2 = \phi_3 = 0$, and an offset of b =−30 mV. The resulting protocol is called 'squarewave' and is shown in Figure 6.

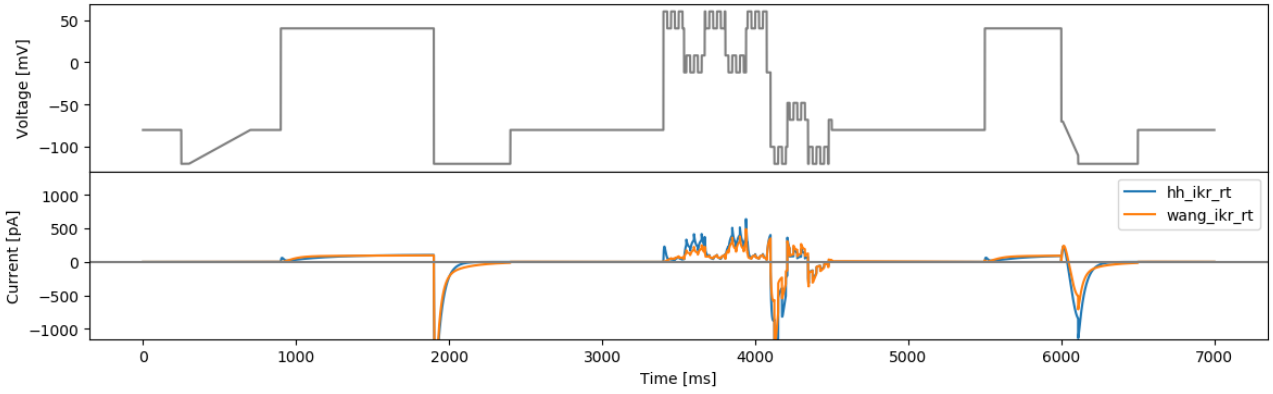

Figure 6: The square wave protocol of Beattie et al. (2018) (squarewave) and simulated currents from both models.

4.5 Long action potential protocol

As a final 'manually-chosen' design, we also propose a lumped action potential protocol for validation purposes, as shown in Figure 7. It consists of two action potential morphologies, an early after-depolarisation (EAD)-like action potential, and a delayed after-depolarisation (DAD)-like action potential. The details of this longap protocol are provided in Table 6.

5 Automated Iterative 3-step designs

Here we describe protocol design approaches that can be done objectively and automatically. With the same rationale as described in Mirams et al. (2024), we consider a protocol consists of $3N$ steps with

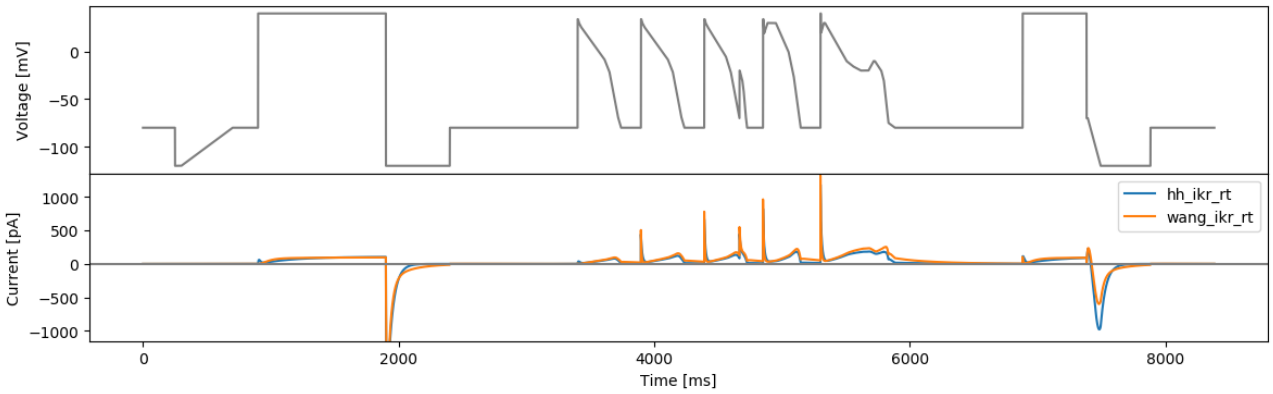

Figure 7: The lumped action potential protocol (longap) and simulated currents from both models.

$N \in \mathbb{N}$, and we split the protocol into N units with 3 consecutive voltage steps as a unit. For some designs, N is the number of model parameters, while for others, N is 17 to bring the total number of steps to 51 which is close to the 64 allowed by the Nanion SyncroPatch384PE when the start and end clamps are added (Table 2). For each unit i, we optimise the 3 voltage steps through an objective function S_i, with each step defined by two parameters: voltage V and duration Δt. Each objective function S_i (described in the sections below) aims to achieve a different purpose. We then iterate the process for all the objective functions $i = 1, 2, \cdots, N$, resulting in a $3N$ steps protocol.

The optimisation was performed using a global optimisation scheme, covariance matrix adaptation evolution strategy (CMA-ES, Hansen, 2006) implemented via a Python package PINTS (Clerx et al., 2019b). All optimisation of the designs were repeated 10 times from different randomly varied initial starting points, and the best designs are presented here. Although we do not expect our design would reach the same global optimum as optimising all > 20 steps at once (Mirams et al., 2024), our results still show promising protocol designs. We also tried to perform fitting 6-steps-at-once in Mirams et al. (2024) and showed that both resulted in similar performance. Finally, the presented results are the optimised results rounded to the nearest one decimal place in millisecond and millivolt for practical implementation (Mirams et al., 2024).

The details of the protocols in this section are provided in Tables 4, 5, and 6.

5.1 Sensitivity-based designs

5.1.1 Maximising approximated local sensitivity

For an ion channel current model I with N parameters $p_1, p_2, \ldots, p_N$, we define an objective function for each 3-step unit i that maximises the absolute value of the elasticity $\left|\frac{\partial I}{\partial p_i} p_i\right|$ of the model output I with respect to the parameter p_i while minimising all the absolute value of elasticity of the rest of the parameters. This objective function can be mathematically expressed as

$$S_i(\{V_{i,j}, \Delta t_{i,j}\}_{j=1}^{3}) = \frac{\int_{\Delta t_{i,3}} \left|\frac{\partial I}{\partial p_i} p_i\right| dt}{\sum_k \int_{\Delta t_{i,3}} \left|\frac{\partial I}{\partial p_k} p_k\right| dt}. \tag{4}$$

The sensitivity was calculated using a first-order central difference scheme with δp_i being $0.1\,\% \times p_i$. Note that the integration is only over the last step of the 3 steps, the idea is to allow the first two steps to vary as much as it would need to be to maximise the approximated local sensitivity across the third step (it is fine if there is low sensitivity because of e.g. full inactivation in the first two steps). This has been repeated for both models and the results are shown in Figures 8 and 9.

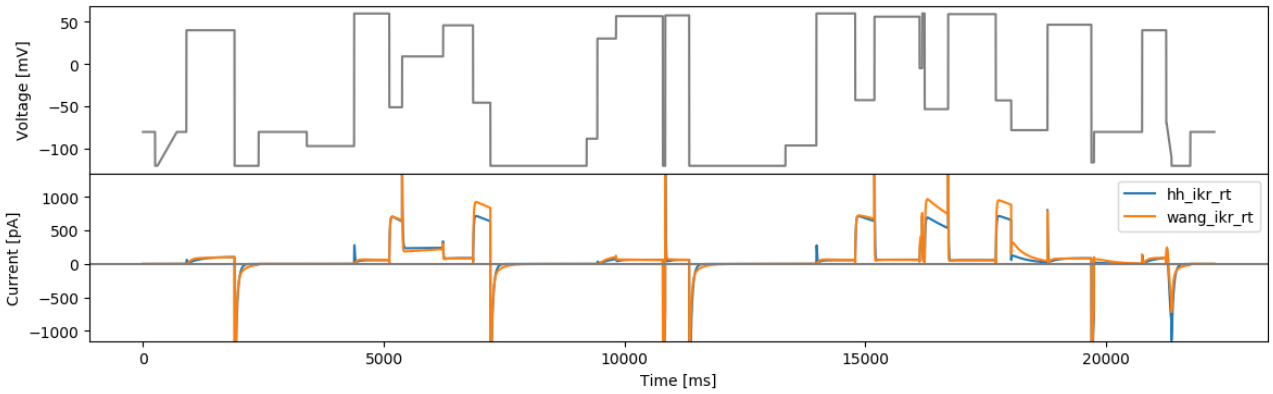

Figure 8: The 3-step local sensitivity protocol based on the Hodgkin-Huxley model (hh3step) and simulated currents from both models.

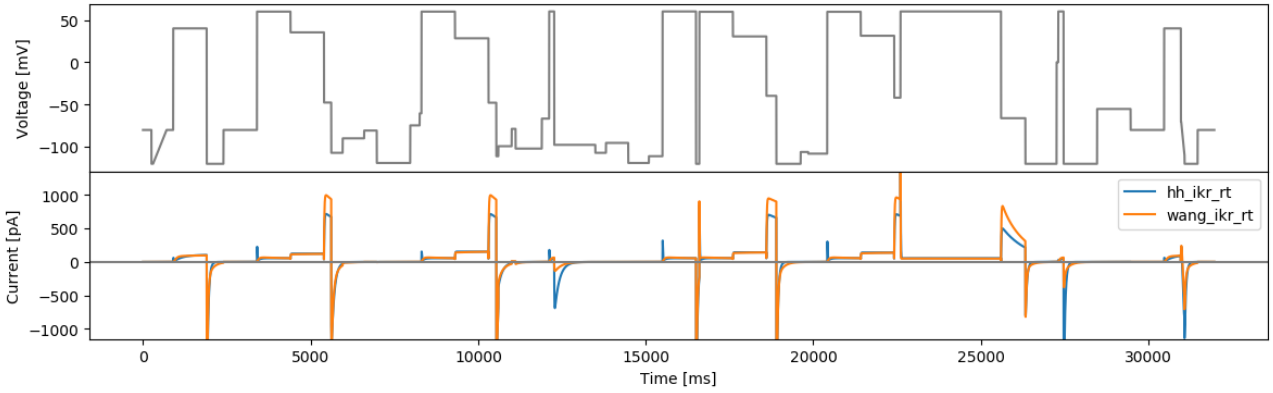

Figure 9: The 3-step local sensitivity protocol based on the Wang model (wang3step) and simulated currents from both models.

5.1.2 Maximising Sobol sensitivity

Instead of the local sensitivity, we can also replace it with the first-order Sobol global sensitivity indices, given by

$$S_i(\{V_{i,j}, \Delta t_{i,j}\}_{j=1}^{3}) = \frac{1}{\mathrm{Var}\,(I)} \mathrm{Var}_{p_i}\left(\mathrm{E}_{p_{!i}}\left(I|p_i\right)\right). \tag{5}$$

Here the $p_{!i}$ notation denotes the set of all parameters except p_i. This has been repeated for the two models described in Section 2. The parameter range (Table 1) was taken from previous real data fits to staircaseramp, sis, hh3step and wang3step, using the approach from Lei et al. (2019b) without accounting for experimental error (Lei et al., 2020a,b).

To calculate Sobol sensitivities we used a modified version of the SA-lib library (Herman and Usher, 2017), to enable easier calculation of sensitivities over time series, which is included in our repository (see Data Availability). The results are shown in Figure 10 and 11.

5.2 Phase-voltage space filling designs

For details of this approach, see Mirams et al. (2024). Briefly, an objective function tries to maximise the amount of new boxes that are visited by a model's trajectory for each new iterative '3 step' set of pulses (as described in Section 4.3) repeating sequentially until we have 17 sets of 3 steps. This approach has a stochastic optimisation step, and produces some protocols that appear to be challenging and information rich, where we appear to have a reasonable amount of current and interesting dynamics. After 30 optimisation runs with different random seeds and initial guesses, we selected the following 3 best protocols based on slightly different criteria:

- Figure 12 — Number 26: the best spcae-filling objective function score (Mirams et al., 2024).

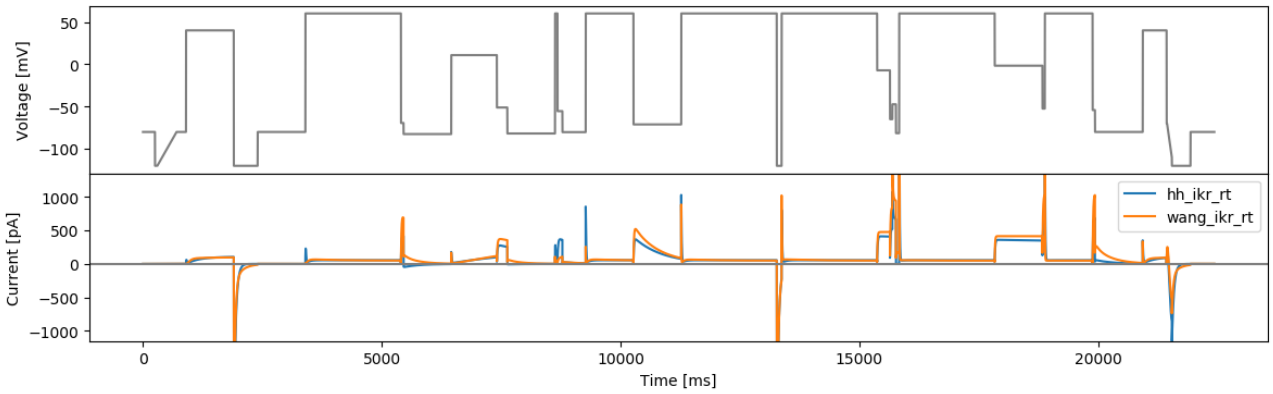

Figure 10: The 3-step Sobol sensitivity protocol based on the Hodgkin-Huxley model (hhsobol3step) and simulated currents from both models.

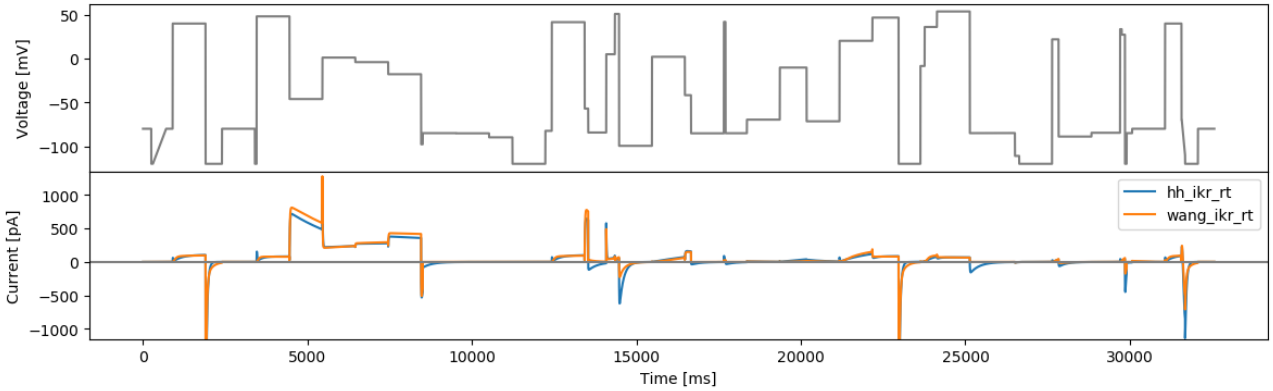

Figure 11: The 3-step Sobol sensitivity protocol based on the Wang model (wangsobol3step) and simulated currents from both models.

- Figure 13 — Number 10: the best score for the RMSD value between the two models described in Section 2 as in Section 5.3.2.
- Figure 14 — Number 19: the best brute-force sampling score (Section 5.3.1) for the Beattie et al. (2018) model.

All three protocols visit between 126–132 (58–61%) of the available 216 'boxes' in phase-voltage space. Note that this is a lower percentage than the protocols in Mirams et al. (2024) primarily due to 1 ms time samples being used in the 2019 optimisations presented here (see Discussion of Mirams et al. (2024)) along with extra initial guesses now being used in the Mirams et al. (2024) optimisation procedure to gain slightly higher coverage of the space.

5.3 Gibbs designs

We use the 3-step approach discussed above, but the difference here is that instead of defining each step by two parameters (voltage V and duration Δt), for each 3-step section we optimise only one of these parameters (either V or Δt) while randomly picking the other from a uniform distribution. This halves the number of parameters that are inferred to just 3 per 3-step section. However, since we have only the same objective function, all units would return the same optimum (or a few if multi-modal but very limited) which is not desired. Therefore we introduce some stochasticity to the protocol by randomly choosing one of the step parameters and optimising only the other one.

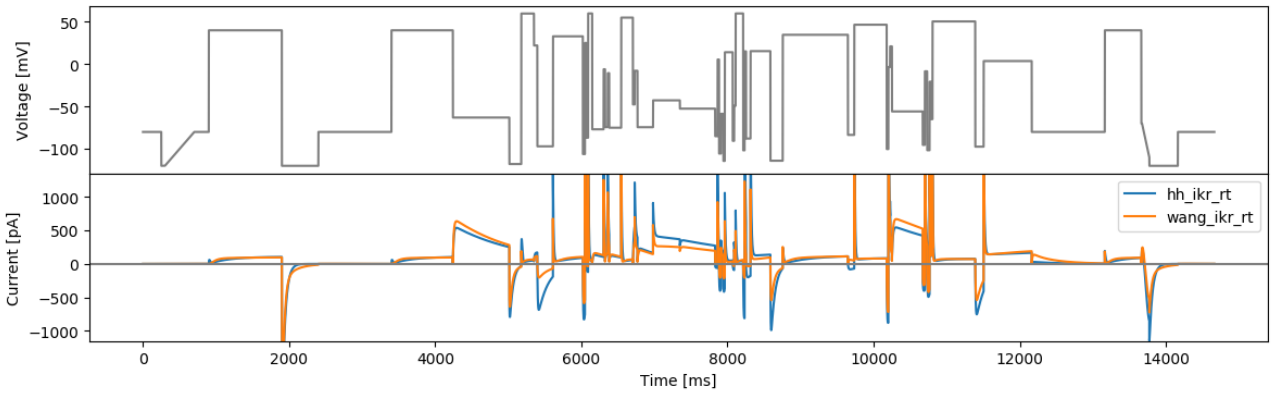

Figure 12: The first phase-voltage space protocol (spacefill26) and simulated currents from both models.

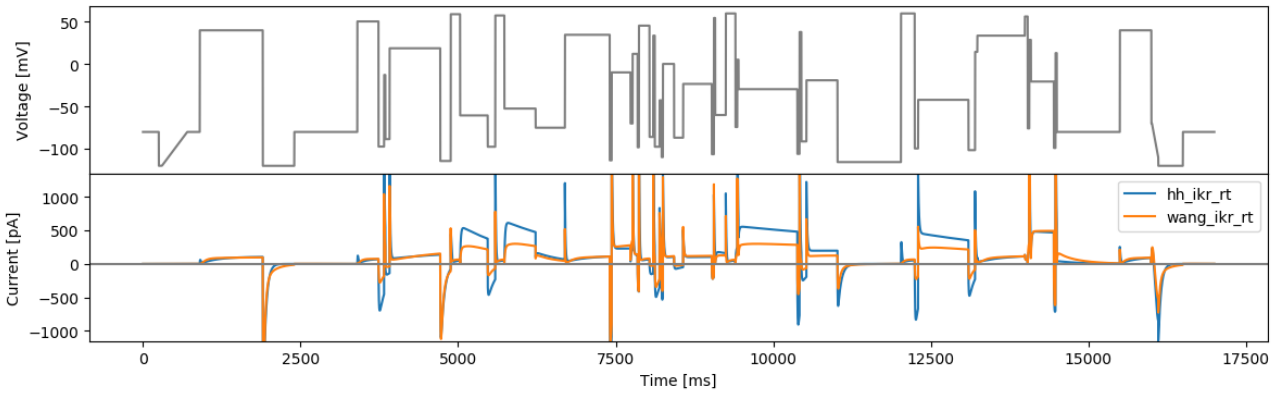

Figure 13: The second phase-voltage space protocol (spacefill10) and simulated currents from both models.

5.3.1 Maximising model output differences: a brute-force sampling approach

The approach taken in this design is similar to a global sensitivity analysis. For a given model I, we start with randomly picking M (ideally $\sim$ 1000s but practically $\sim$ 100s of) parameters from model parameter prior, then the objective function to be optimised is the sum of the root mean square deviation (RMSD) values between the model outputs from all combinations of the sampled parameter pairs. The model parameter prior could be an a-priori distribution of the parameters (for example those used in Beattie et al., 2018; Lei et al., 2019b), or based on previous fitting results (see below). The objective function for a 3-step unit i can be expressed as

$$S(\boldsymbol{\theta}_i) = \frac{2}{M^2} \sum_{j=1}^{M} \sum_{k>j}^{M} \text{RMSD}(I_j, I_k), \tag{6}$$

where $\text{RMSD}(x, y)$ denotes the RMSD between x and y, and I_j, I_k are the model output for the M parameter samples. We choose $\boldsymbol{\theta}_i = \{V_j\}_{j=1}^{3}$ with $\Delta t_j \sim \text{Uniform}(50, 1000)$ ms for odd i, and $\boldsymbol{\theta}_i = \{\Delta t_j\}_{j=1}^{3}$ with $V_j \sim \text{Uniform}(-120, 60)$ mV for even i.

This has been repeated for the two models described in Section 2, and the parameter range (prior distribution) was taken from the maximum range defined by previous real data fits to staircsaeramp, sis, hh3step and wang3step, as provided in Table 1. The results are shown in Figure 15 and 16.

5.3.2 Maximising differences between two models

Unlike the previously defined approaches, where only one model was involved, this proposed approach aims to distinguish between two candidate models. The objective function is defined as the RMSD

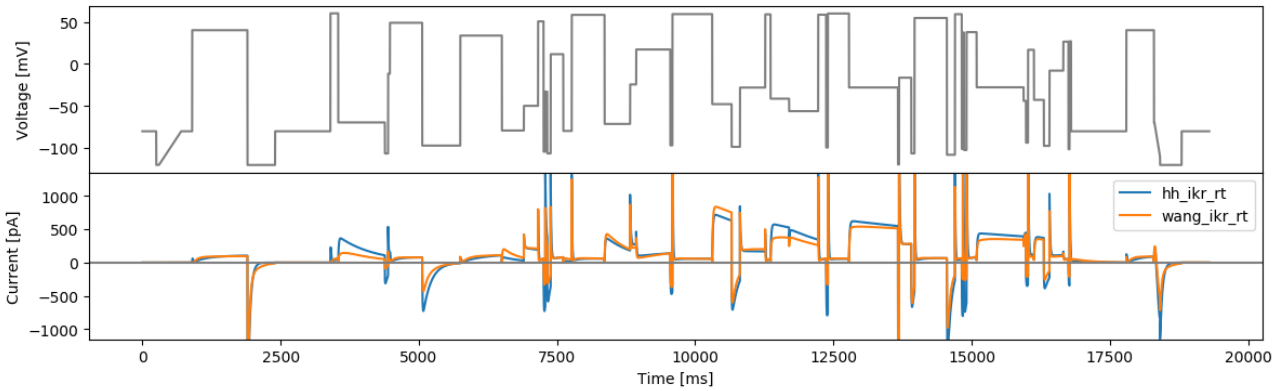

Figure 14: The third phase-voltage space protocol (spacefill19) and simulated currents from both models.

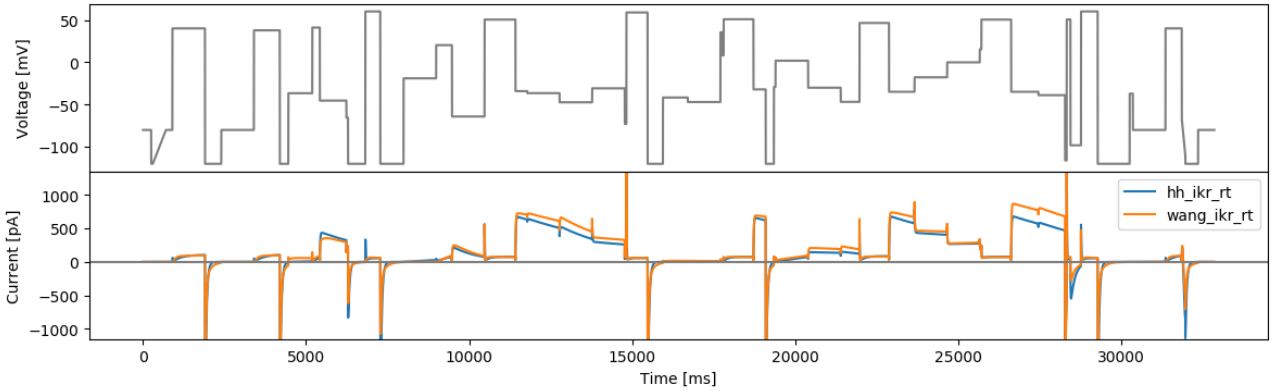

Figure 15: The brute-force sampling protocol based on the Hodgkin-Huxley model (hhbrute3gstep) and simulated currents from both models.

value between two model currents, with a given set of model parameters (Table 1), so it is still a 'local' design with respect to model parameters. One protocol randomly picks time parameters for each 3-step unit, and optimises voltages ($\{V_j\}_{j=1}^3$ with $\Delta t_j \sim \text{Uniform}(50, 500)$ ms and is termed 'rtovmaxdiff'); and the other method randomly picks voltages and optimises the step durations $\{\Delta t_j\}_{j=1}^3$ with $V_j \sim \text{Uniform}(-120, 60)$ mV, and is known as 'rvotmaxdiff'. Applying this approach to the two models described in Section 2 results in Figures 17 and 18.

6 Automated square waves

Following the same argument as in Section 5.3.2, this design maximises the differences between two candidate models to aid model selection. Here we use $N = 3$ (as per Beattie et al., 2018) which gives 9 parameters in total (see Equation (3)), with a fixed offset voltage of -30 mV. The square wave parameters are optimised based on an objective function that maximises the RMSD value between two model outputs. Similar to Section 5.3.2, the two models have a set of predefined model parameters, so it is still a 'local' model parameter method.

This approach was applied to the two models described in Section 2 using the original model parameters. The resulting protocol (Figure 19) exhibits extremely high frequency and high amplitude (hitting the boundaries of the protocol parameters) behaviour. We believe these rapid changes of voltage tends to maximise the two model outputs, which is similar to the 'original sine wave #2' in Beattie (2015), and is likely to be impractical or uninformative for real experiments.

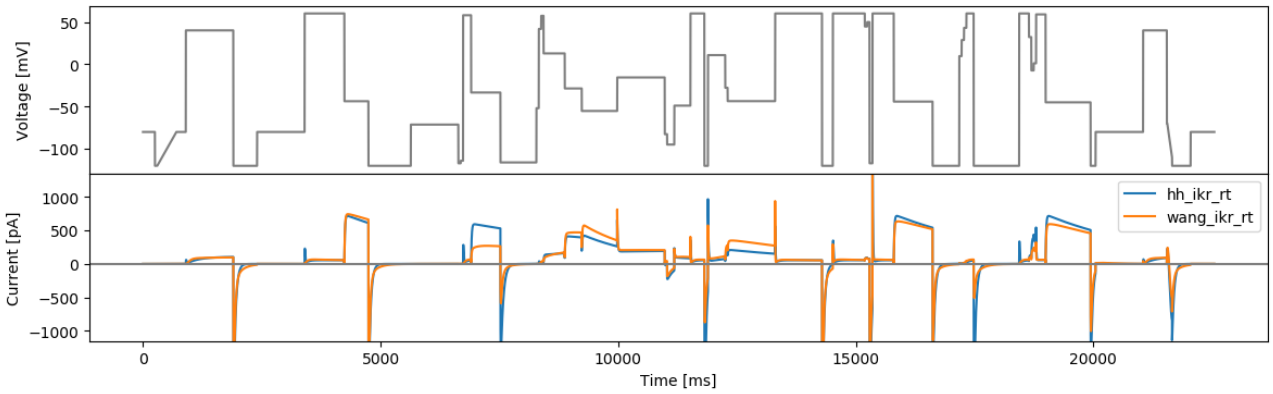

Figure 16: The brute-force sampling protocol based on the Wang model (wangbrute3gstep) and simulated currents from both models.

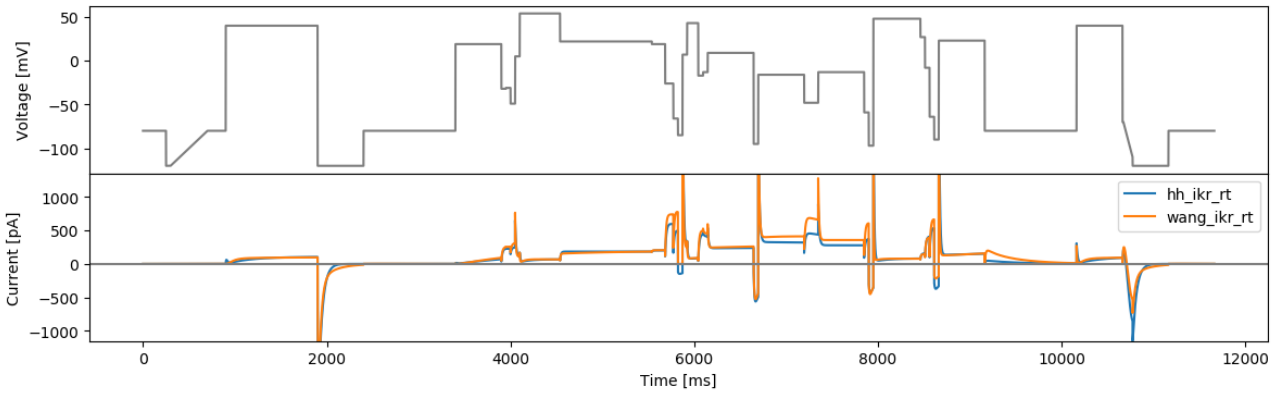

Figure 17: Protocol rvotmaxdiff and simulated currents from both models.

7 Discussion

Developing ion channel models remains a challenging task predominantly due to all the various sources of uncertainty and variability (Mirams et al., 2016) — in terms of modelling approximations (Lei et al., 2020c; Lei and Mirams, 2021) as well as experimental noise and artefacts (Lei et al., 2020a). It is made more difficult due to the sparsity of available data for independent training and validation, with it still being common to calibrate models to all available data (Whittaker et al., 2020). The protocols presented here encompass many design criteria, including parameterisation, model selection and rigorous testing of the underlying assumptions in hERG models (Fink and Noble, 2009; Lei et al., 2019b; Mirams et al., 2024). As such, we expect that this collection of voltage clamp protocols will be extremely useful for development of mathematical models for the physiological gating of the hERG potassium channel, and in particular by providing ample validation data for assessing their prediction errors due to model discrepancy (Shuttleworth et al., 2024).

The same design criteria we have outlined here could easily be applied to other ion channels to create similar suites of protocols, using the provided open source codes.

Data Availability

Open source code to reproduce the protocols in this report can be found on GitHub:
`https://github.com/CardiacModelling/protocol-design-hERG`

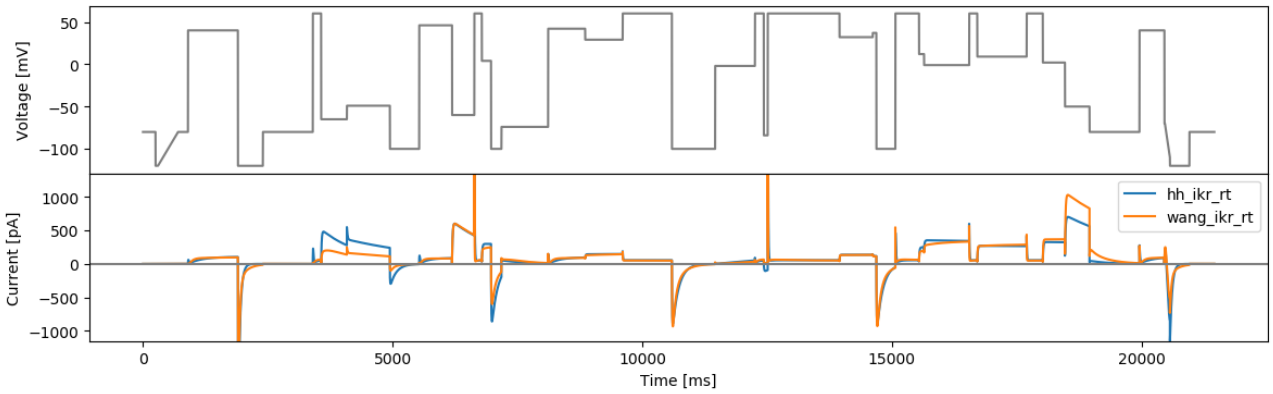

Figure 18: Protocol rtovmaxdiff and simulated currents from both models.

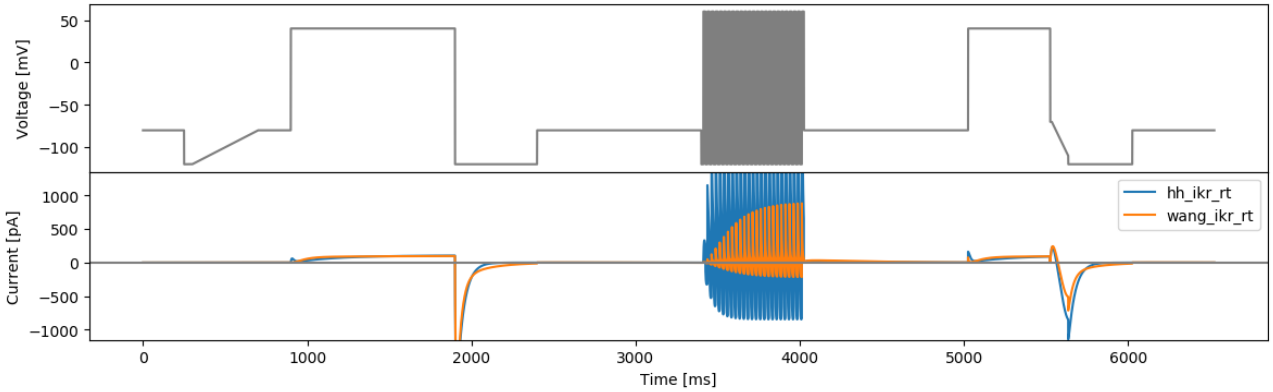

Figure 19: The square wave protocol for maximising two models' difference (maxdiff) and simulated currents from both models.

Acknowledgements

This work was supported by the Wellcome Trust (grant no. 212203/Z/18/Z); the Science and Technology Development Fund, Macao SAR (FDCT) [reference no. 0155/2023/RIA3 and 0048/2022/A]; the University of Macau [reference no. SRG2024-00014-FHS and FHS Startup Grant]; the Engineering & Physical Sciences Research Council (EPSRC) [grant no. EP/R014604/1]; and the Australian Research Council [grant no. DP190101758]. DGW & GRM acknowledge support from the Wellcome Trust via a Wellcome Trust Senior Research Fellowship to GRM. CLL acknowledges support from the FDCT and support from the University of Macau. We acknowledge Victor Chang Cardiac Research Institute Innovation Centre, funded by the NSW Government. The authors would like to thank the Isaac Newton Institute for Mathematical Sciences for support and hospitality during the programme The Fickle Heart when some work on this report was undertaken, and in particular discussions with Prof. Ian Vernon.

This research was funded in whole, or in part, by the Wellcome Trust [212203/Z/18/Z]. For the purpose of open access, the authors have applied a CC-BY public copyright licence to any Author Accepted Manuscript version arising from this submission.

References

Beattie, K. (2015). *Mathematical modelling of drug-ion channel interactions for cardiac safety assessment*. PhD thesis, University of Oxford.

Beattie, K. A., Hill, A. P., Bardenet, R., Cui, Y., Vandenberg, J. I., Gavaghan, D. J., Boer, T. P. d., and Mirams, G. R. (2018). Sinusoidal voltage protocols for rapid characterisation of ion channel kinetics. *The Journal of Physiology*, 596(10):1813–1828.

Bett, G. C., Zhou, Q., and Rasmusson, R. L. (2011). Models of HERG gating. *Biophysical Journal*, 101(3):631–642.

Clerx, M., Beattie, K. A., Gavaghan, D. J., and Mirams, G. R. (2019a). Four ways to fit an ion channel model. *Biophysical Journal*, 117(12):2420–2437.

Clerx, M., Collins, P., De Lange, E., and Volders, P. G. (2016). Myokit: a simple interface to cardiac cellular electrophysiology. *Progress in Biophysics and Molecular Biology*, 120(1-3):100–114.

Clerx, M., Robinson, M., Lambert, B., Lei, C. L., Ghosh, S., Mirams, G. R., and Gavaghan, D. J. (2019b). Probabilistic inference on noisy time series (PINTS). *Journal of Open Research Software*, 7:23.

Fink, M. and Noble, D. (2009). Markov models for ion channels: versatility versus identifiability and speed. *Philosophical Transactions of the Royal Society A: Mathematical, Physical and Engineering Sciences*, 367(1896):2161–2179.

Fink, M., Noble, D., Virag, L., Varro, A., and Giles, W. R. (2008). Contributions of hERG K+ current to repolarization of the human ventricular action potential. *Progress in Biophysics and Molecular Biology*, 96(1-3):357–376.

Hansen, N. (2006). *The CMA Evolution Strategy: A Comparing Review*, pages 75–102. Springer Berlin Heidelberg, Berlin, Heidelberg.

Herman, J. and Usher, W. (2017). SALib: An open-source Python library for sensitivity analysis. *Journal of Open Source Software*, 2(9):97.

Hindmarsh, A. C., Brown, P. N., Grant, K. E., Lee, S. L., Serban, R., Shumaker, D. E., and Woodward, C. S. (2005). SUNDIALS: Suite of nonlinear and differential/algebraic equation solvers. *ACM Transactions on Mathematical Software (TOMS)*, 31(3):363–396.

Lei, C. L., Clerx, M., Beattie, K. A., Melgari, D., Hancox, J. C., Gavaghan, D. J., Polonchuk, L., Wang, K., and Mirams, G. R. (2019a). Rapid characterization of hERG channel kinetics II: temperature dependence. *Biophysical Journal*, 117(12):2455–2470.

Lei, C. L., Clerx, M., Gavaghan, D. J., and Mirams, G. R. (2023). Model-driven optimal experimental design for calibrating cardiac electrophysiology models. *Computer Methods and Programs in Biomedicine*, 240:107690.

Lei, C. L., Clerx, M., Gavaghan, D. J., Polonchuk, L., Mirams, G. R., and Wang, K. (2019b). Rapid characterization of hERG channel kinetics I: using an automated high-throughput system. *Biophysical Journal*, 117(12):2438–2454.

Lei, C. L., Clerx, M., Whittaker, D. G., Gavaghan, D. J., de Boer, T. P., and Mirams, G. R. (2020a). Accounting for variability in ion current recordings using a mathematical model of artefacts in voltage-clamp experiments. *Philosophical Transactions of the Royal Society A*, 378(2173):20190348.

Lei, C. L., Fabbri, A., Whittaker, D. G., Clerx, M., Windley, M. J., Hill, A. P., Mirams, G. R., and de Boer, T. P. (2020b). A nonlinear and time-dependent leak current in the presence of calcium fluoride patch-clamp seal enhancer. *Wellcome Open Research*, 5.

Lei, C. L., Ghosh, S., Whittaker, D. G., Aboelkassem, Y., Beattie, K. A., Cantwell, C. D., Delhaas, T., Houston, C., Novaes, G. M., Panfilov, A. V., et al. (2020c). Considering discrepancy when calibrating a mechanistic electrophysiology model. *Philosophical Transactions of the Royal Society A*, 378(2173):20190349.

Lei, C. L. and Mirams, G. R. (2021). Neural network differential equations for ion channel modelling. *Frontiers in Physiology*, 12:708944.

Mirams, G. R. (2023). Computational cardiac safety testing. In *Drug Discovery and Evaluation: Safety and Pharmacokinetic Assays*, pages 1–33. Springer.

Mirams, G. R., Clerx, M., Whittaker, D. G., and Lei, C. L. (2024). Optimal experimental designs for characterising ion channel gating by filling the phase-voltage space of model dynamics. *Mathematics in Medical and Life Sciences*, 1(1):2375494.

Mirams, G. R., Niederer, S. A., and Clayton, R. H. (2020). The fickle heart: uncertainty quantification in cardiac and cardiovascular modelling and simulation. *Philosophical Transactions of the Royal Society A*, 378(2173):20200119.

Mirams, G. R., Pathmanathan, P., Gray, R. A., Challenor, P., and Clayton, R. H. (2016). Uncertainty and variability in computational and mathematical models of cardiac physiology. *The Journal of Physiology*, 594(23):6833–6847.

Obergrussberger, A., Brüggemann, A., Goetze, T. A., Rapedius, M., Haarmann, C., Rinke, I., Becker, N., Oka, T., Ohtsuki, A., Stengel, T., Vogel, M., Steindl, J., Mueller, M., Stiehler, J., George, M., and Fertig, N. (2016). Automated patch clamp meets high-throughput screening: 384 cells recorded in parallel on a planar patch clamp module. *Journal of Laboratory Automation*, 21(6):779–793.

Rudy, Y. and Silva, J. R. (2006). Computational biology in the study of cardiac ion channels and cell electrophysiology. *Quarterly Reviews of Biophysics*, 39(1):57–116.

Sanguinetti, M. C., Jiang, C., Curran, M. E., and Keating, M. T. (1995). A mechanistic link between an inherited and an acquird cardiac arrthytmia: hERG encodes the IKr potassium channel. *Cell*, 81(2):299–307.

Shuttleworth, J. G., Lei, C. L., Whittaker, D. G., Windley, M. J., Hill, A. P., Preston, S. P., and Mirams, G. R. (2024). Empirical quantification of predictive uncertainty due to model discrepancy by training with an ensemble of experimental designs: an application to ion channel kinetics. *Bulletin of Mathematical Biology*, 86(1):2.

Vandenberg, J. I., Perry, M. D., Perrin, M. J., Mann, S. A., Ke, Y., and Hill, A. P. (2012). hERG K+ channels: structure, function, and clinical significance. *Physiological Reviews*, 92:1393–1478.

Wang, S., Liu, S., Morales, M. J., Strauss, H. C., and Rasmusson, R. L. (1997). A quantitative analysis of the activation and inactivation kinetics of hERG expressed in Xenopus oocytes. *The Journal of Physiology*, 502(1):45–60.

Whittaker, D. G., Clerx, M., Lei, C. L., Christini, D. J., and Mirams, G. R. (2020). Calibration of ionic and cellular cardiac electrophysiology models. *Wiley Interdisciplinary Reviews: Systems Biology and Medicine*, 12(4):e1482.

Table 3: Details of the 5 protocols: staircase, sis, sisi, manualppx, and squarewave. All voltage values shown here are voltage steps to clamp to. These steps need to have the two 'bookend' sections added (see Table 2) which are identical for all designs.

Clamp	staircase		sis		sisi		manualppx		squarewave	
#	V (mV)	t (ms)	V (mV)	t (ms)	V (mV)	t (ms)	V (mV)	t (ms)	V (mV)	t (ms)
1	-40	500	-40	500	40	500	60	200	60	24.9
2	-60	500	-60	500	0	500	-60	200	40	25
3	-20	500	-20	500	20	500	-100	200	60	25
4	-40	500	-40	500	-20	500	40	500	40	25
5	0	500	0	500	0	500	-90	200	60	25.1
6	-20	500	-20	500	-40	500	30	500	40	9.9
7	20	500	20	500	-20	500	-80	200	-12	15
8	0	500	0	500	-60	500	-100	200	8	25.1
9	40	500	40	225	-40	225	20	200	-12	24.9
10	20	500	-80	50	-80	50	-40	1000	8	25
11	40	500	-40	50	-40	50	60	200	-12	25.1
12	0	500	-60	50	-60	50	0	200	8	19.9
13	20	500	-20	50	-20	50	-50	1000	60	5
14	-20	500	-40	50	-40	50	-10	100	40	25
15	0	500	0	50	0	50	10	100	60	25.1
16	-40	500	-20	50	-20	50	-20	100	40	25
17	-20	500	20	50	20	50	-80	300	60	25
18	-60	500	0	50	0	50	0	100	40	24.9
19	-40	500	40	50	40	50	-20	100	60	5
20	—	—	20	50	20	50	-100	200	8	20.1
21			40	50	40	50	40	300	-12	24.9
22			0	50	0	50	-60	100	8	25
23			20	50	20	50	0	100	-12	25.1
24			-20	50	-20	50	-10	100	8	24.9
25			0	50	0	50	-20	100	-12	15
26			-40	50	-40	50	-30	100	40	10
27			-20	50	-20	50	-40	100	60	25.1
28			-60	50	-60	50	-80	100	40	24.9
29			-40	50	-40	50	30	100	60	25
30			-80	50	-80	50	60	100	40	25.1
31			40	225	-40	225	—	—	60	24.9
32			0	500	-60	500			-12	25.1
33			20	500	-20	500			-100	25
34			-20	500	-40	500			-120	25
35			0	500	0	500			-100	25
36			-40	500	-20	500			-120	24.9
37			-20	500	20	500			-100	10
38			-60	500	0	500			-48	15
39			-40	500	40	500			-68	25.1
40			—	—	—	—			-48	25
41									-68	24.9
42									-48	25
43									-68	20
44									-120	5
45									-100	25
46									-120	25.1
47									-100	25
48									-120	24.9
49									-100	25.1
50									-120	4.9
51									-68	20

Table 4: Details of the 5 protocols: hh3step, wang3step, hhsobol3step, wangsobol3step, and spacefill26. All voltage values shown here are voltage steps to clamp to. These steps need to have the two 'bookend' sections added (see Table 2) which are identical for all designs.

Clamp	hh3step		wang3step		hhsobol3step		wangsobol3step		spacefill26	
#	V (mV)	t (ms)	V (mV)	t (ms)	V (mV)	t (ms)	V (mV)	t (ms)	V (mV)	t (ms)
1	-96.7	983	59.8	1000	60	1000	-120	52.8	40	841
2	59.7	730	35.3	1000	60	1000	48.2	1000	-63	773
3	-50.9	266	-47.6	216	-69.4	54.9	-46.1	1000	-117.9	163
4	9.07	852	-107	341	-82.5	999	1.3	1000	59.8	174
5	45.8	621	-89.9	641	10.8	955	-4.03	1000	22.1	46
6	-45.5	360	-80.7	377	-51.1	219	-17.8	1000	-97	214
7	-120	999	-119	998	-81.8	999	-97.7	50.4	32.9	409
8	-120	1000	-74.6	281	60	51.5	-85	784	-106.1	29
9	-88	222	-60.4	54.4	-55.4	103	-85	232	25.1	20
10	30.2	388	59.8	1000	-80.2	488	-85.2	1000	-86.8	23
11	56.6	972	28.3	1000	60	1000	-89.8	711	59.9	56
12	-120	50.2	-47.8	233	-71.1	1000	-120	1000	-76.9	156
13	57.5	497	-111	61.2	60	1000	-82.4	195	-6	20
14	-120	1000	-99.2	398	60	1000	41.6	1000	-74.3	37
15	-120	999	-78.7	116	-120	102	-57	108	-10.6	20
16	-96	642	-102	783	60	1000	-84.3	548	-75	164
17	59.8	806	-66.6	219	60	1000	5.02	261	55	160
18	-42.5	400	60	151	-7.19	269	51	129	-47.5	25
19	56	936	-97.6	443	-64.9	50	-99.5	1000	-7.8	38
20	-4.8	55.6	-97.6	784	-47.3	75.1	2.12	1000	-74.4	213
21	59.8	50	-107	317	-81.4	67.3	-41.7	187	-42.7	367
22	-53.1	488	-95.3	665	60	1000	-85.2	999	-52.5	483
23	59	989	-119	616	60	1000	41.9	50.2	-85	33
24	-42.8	321	-111	407	-1.7	1000	-85.1	650	5.5	20
25	-77.9	753	60	1000	-52.4	50	-69.6	1000	-105.5	27
26	46.5	911	-120	50	60	1000	-10.2	815	-58.6	32
27	-116	54.3	-120	50	-54.1	50	-71.5	1000	-114.2	20
28	—	—	59.6	1000	—	—	20.3	1000	14.1	108
29			30.5	1000			46.8	797	-90.5	20
30			-39.7	297			-120	663	-49.1	20
31			-120	725			-8.4	128	59.9	103
32			-106	225			36.1	374	-101.7	20
33			-108	568			53.8	999	15.1	20
34			59.6	1000			-85	949	-87.8	61
35			31.3	999			-84.9	423	15.4	272
36			-41.9	187			-111	129	-114	169
37			60	1000			-120	1000	34.7	892
38			60	1000			22	198	-83.5	87
39			60	1000			-88.9	1000	46.6	444
40			-66.1	727			-84.6	869	-100.2	23
41			-120	931			33.6	50	-3.3	23
42			0	50			27.3	99.3	21	26
43			60	159			-120	50.3	-55.8	421
44			-120	1000			-85	107	-95.3	29
45			-55.2	1000			-85	60.7	-8.4	32
46			—	—			—	—	-101.6	33
47									-20.7	20
48									-64.9	20
49									50.5	585
50									-97.4	115
51									3.7	658

Table 5: Details of the 5 protocols: spacefill10, spacefill19, hhbrute3gstep, wangbrute3gstep, and rvotmaxdiff. All voltage values shown here are voltage steps to clamp to. These steps need to have the two 'bookend' sections added (see Table 2) which are identical for all designs.

Clamp	spacefill10		spacefill19		hhbrute3gstep		wangbrute3gstep		rvotmaxdiff	
#	V (mV)	t (ms)	V (mV)	t (ms)	V (mV)	t (ms)	V (mV)	t (ms)	V (mV)	t (ms)
1	50.5	336	60	142	37.7	795	60	837	19	500
2	-97.3	89	-69.5	844	-120	261	-43.7	506	-32	50
3	-12.7	20	-106.3	58	-36.6	735	-120	892	-31	50
4	-88.5	67	-11.6	33	41	231	-71.3	1000	-49	50
5	18.8	804	48.8	584	-45.3	815	-117	50	5	50
6	-114.3	166	-97	689	-65.4	50.2	-114	50	54	439
7	59	149	33.6	752	-120	530	57.9	169	22	499
8	-60.5	438	-79.1	398	60	459	-33.4	617	22	500
9	-97.5	120	-49.8	257	-120	714	-116	757	19	145
10	57.5	144	50.5	99	-19	1000	-51.9	50	-26	89
11	-52.4	496	-104.2	32	20.2	485	41.7	50	-66	50
12	-75	465	-33	35	-64.1	1000	57.2	50.4	-85	50
13	34.7	711	-106.3	62	50.4	947	12.8	446	7	50
14	-113.5	31	11.5	228	-34.1	362	-28.6	358	43	121
15	-9.7	299	-79.6	153	-36.5	991	-55.2	746	-17	53
16	-70	33	58.2	594	-47.3	1000	-15.6	1000	-13	50
17	12.2	79	-71.3	462	-30.8	1000	-82.6	50	9	500
18	-98.1	21	-24.4	110	-72.9	50.1	-94.9	152	-95	50
19	45.5	168	17.1	617	58.8	650	-48.9	339	-16	500
20	-85.9	59	-96.7	38	-120	471	60	293	-48	153
21	33.7	25	59.1	720	-41.7	762	-120	76.3	-13	500
22	-97.5	76	-47.8	351	-47	1000	10.8	363	-59	50
23	-42.7	32	-98.5	151	35.4	50	-27.8	50.5	-97	50
24	-109.7	21	-28.1	457	8.1	50	-43.6	1000	48	460
25	0.3	177	58.8	96	50.8	914	60	986	48	52
26	-86.8	144	-41.3	336	-32.1	376	-120	228	27	50
27	-23.3	455	-56.1	526	-120	251	60	672	-8	50
28	-106.3	33	58.4	144	-29.2	50	44.6	50	-64	50
29	54.6	20	-99.3	31	1.81	1000	49.8	50	-90	50
30	-60	169	59.8	382	-30.1	1000	-117	62.2	23	500
31	59.9	153	-28	886	-46.8	576	60	448	—	—
32	-74.2	29	-119.4	20	46.4	905	-44.1	817		
33	5.3	20	-16.4	221	-34.9	783	-120	561		
34	-29.5	933	-106.3	58	-17.8	1000	9.6	50		
35	-105.9	35	54.5	586	-0.1	1000	28.6	50		
36	38	29	-107.9	146	15.3	50	43	50.4		
37	-91.2	80	59	123	50.4	913	60	153		
38	-19	493	-101	21	-34.9	835	-120	957		
39	-115.6	1007	37.2	20	-38.9	818	60	206		
40	59.9	218	-102.3	46	-116	50.5	32.1	50		
41	-99.5	54	37.7	182	50.5	115	-7.3	50.5		
42	-42.1	799	-27.8	849	-98.1	324	1.1	50		
43	-101.5	105	-43.9	44	60	512	58.9	200		
44	14.5	36	-93.5	37	-120	980	-45	947		
45	33.7	754	16.7	107	-37.1	98.9	-120	105		
46	56.3	45	-42.7	179	—	—	—	—		
47	-75.8	25	-97.3	102						
48	28.7	26	-8	250						
49	-20.5	364	26.4	93						
50	-98.9	26	-101.3	20						
51	13.1	21	26.8	27						

Table 6: Details of the 3 protocols: rtovmaxdiff, maxdiff, and longap. All voltage values for protocols rtovmaxdiff and maxdiff are voltage steps to clamp to. Protocol longap also indicates with 'Ramp' or 'Step'; 'Ramp' is specified it is a linear ramp over time between the voltages shown, as opposed to a constant voltage clamp for a 'Step'. These steps need to have the two 'bookend' sections added (see Table 2) which are identical for all designs.

Clamp	rtovmaxdiff		maxdiff		longap		
#	V (mV)	t (ms)	V (mV)	t (ms)	Step/Ramp	V (mV)	t (ms)
1	60	167	-120	12.5	Step	34	3
2	-65	516	60	12.5	Ramp	30	8
3	-49	861	-120	12.5	Ramp	26	15.2
4	-100	587	60	12.5	Ramp	-8	183.6
5	46	658	-120	12.5	Ramp	-21	39
6	-60	446	60	12.5	Ramp	-68	65.8
7	60	150	-120	12.5	Ramp	-80	25.2
8	4	185	60	12.5	Step	-80	155.6
9	-100	208	-120	12.5	Step	34	3
10	-74	935	60	12.5	Ramp	30	8
11	42	742	-120	12.5	Ramp	26	15.2
12	29	751	60	12.5	Ramp	-8	183.6
13	60	986	-120	12.5	Ramp	-21	39
14	-100	866	60	12.5	Ramp	-68	65.8
15	-2	797	-120	12.5	Ramp	-80	25.2
16	60	177	60	12.5	Step	-80	155.6
17	-84	79	-120	12.5	Step	34	3
18	60	943	60	12.5	Ramp	30	8
19	60	494	-120	12.5	Ramp	26	15.2
20	32	666	60	12.5	Ramp	-5	142.6
21	37	73	-120	12.5	Ramp	-21	38.4
22	-100	380	60	12.5	Ramp	-70	68.6
23	60	474	-120	12.5	Step	-20	2
24	12	101	60	12.5	Ramp	-30	20
25	-1	904	-120	12.5	Ramp	-40	10
26	60	162	60	12.5	Ramp	-65	15
27	9	989	-120	12.5	Ramp	-80	12
28	60	323	60	12.5	Step	-80	125
29	2	444	-120	12.5	Step	34	3
30	-50	492	60	12.5	Ramp	19	6
31	—	—	-120	12.5	Ramp	30	26.4
32			60	12.5	Step	30	65
33			-120	12.5	Ramp	0	99
34			60	12.5	Ramp	-25	40
35			-120	12.5	Ramp	-80	55
36			60	12.5	Step	-80	155
37			-120	12.5	Step	40	3
38			60	12.5	Step	20	3
39			-120	12.5	Ramp	30	20
40			60	12.5	Step	30	10
41			-120	12.5	Ramp	-10	168
42			60	12.5	Ramp	-15.5	50.6
43			-120	12.5	Ramp	-20	61.2
44			60	12.5	Step	-20	60
45			-120	12.5	Ramp	-10	40
46			60	12.5	Step	-10	10
47			-120	12.5	Ramp	-20	50
48			60	12.5	Ramp	-30	20
49			-120	12.5	Ramp	-75	36
50			60	12.5	Ramp	-80	50